Potentiation of Temozolomide Cytotoxicity by Poly(ADP)Ribose Polymerase Inhibitor ABT-888 Requires a Conversion of Single-Stranded DNA Damages to Double-Stranded DNA Breaks

Xuesong Liu,[1] Yan Shi,[1] Ran Guan,[1] Cherrie Donawho,[1] Yanping Luo,[2] Joann Palma,[1] Gui-dong Zhu,[1] Eric F. Johnson,[1] Luis E. Rodriguez,[1] Nayereh Ghoreishi-Haack,[2] Ken Jarvis,[1] Vincent P. Hradil,[2] Milagros Colon-Lopez,[1] Bryan F. Cox,[2] Vered Klinghofer,[1] Thomas Penning,[1] Saul H. Rosenberg,[1] David Frost,[1] Vincent L. Giranda,[1] and Yan Luo[1]

[1]Cancer Research and [2]Advance Technology, GPRD, Abbott Laboratories, Abbott Park, Illinois

Abstract

Poly(ADP-ribose) polymerase (PARP) senses DNA breaks and facilitates DNA repair via the polyADP-ribosylation of various DNA binding and repair proteins. We explored the mechanism of potentiation of temozolomide cytotoxicity by the PARP inhibitor ABT-888. We showed that cells treated with temozolomide need to be exposed to ABT-888 for at least 17 to 24 hours to achieve maximal cytotoxicity. The extent of cytotoxicity correlates with the level of double-stranded DNA breaks as indicated by γH2AX levels. In synchronized cells, damaging DNA with temozolomide in the presence of ABT-888 during the S phase generated high levels of double-stranded breaks, presumably because the single-stranded DNA breaks resulting from the cleavage of the methylated nucleotides were converted into double-stranded breaks through DNA replication. As a result, treatment of temozolomide and ABT-888 during the S phase leads to higher levels of cytotoxicity. ABT-888 inhibits poly(ADP-ribose) formation *in vivo* and enhances tumor growth inhibition by temozolomide in multiple models. ABT-888 is well tolerated in animal models. ABT-888 is currently in clinical trials in combination with temozolomide. (Mol Cancer Res 2008;6(10):1621–9)

Introduction

Poly(ADP-ribose) (PAR) polymerase (PARP) catalyzes the synthesis of PAR, the activity of which was first identified by Chambon et al. more than 40 years ago (1). Eighteen putative PARP family members have been identified thus far and their cellular functions are involved in DNA damage and DNA repair responses, modulation of chromatin structure, transcription regulation, DNA telomere maintenance, mitotic control, cellular transport, and cell death (2-5). PARP-1 and PARP-2 exert important functions in sensing DNA damage and facilitating DNA repair (6-8). PARP-1 preferentially recognizes single-stranded DNA breaks (SSB) caused by oxidative stress, radiation, topoisomerase I (Topo I) inhibitors, alkylating agents, etc. (9). The role of PARP-1 has perhaps been best shown in the base excision repair (BER) process. Whereas PARP-1 has not been shown to function directly in mismatch repair (MMR) or nucleotide excision repair, some of the proteins involved in these processes, such as MSH6 or DNA polymerase ε, bind with PAR via PAR-binding motifs (10). In addition, PARP inhibitors have been shown to restore the sensitivity of MMR-deficient cells to temozolomide (11-13), presumably by interfering with the efficient BER repair of temozolomide-induced damage. Recently, PARP was also shown to be involved in homologous recombination repair and nonhomologous end-joining repair of double-stranded breaks (DSB; refs. 14-16).

Up-regulation of PARP-1 expression or activity has been observed in multiple hematopoetic malignancies and solid tumor types. For example, PARP mRNA levels were found to be enhanced in malignant lymphomas but not in normal lymph nodes or reactive proliferative lymph nodes (17). Elevated PARP activity was identified in peripheral lymphocytes from patients with low-grade malignant non–Hodgkin's lymphoma (18), hepatocellular carcinomas (19, 20), small-cell lung cancer lines (21), cervical cancer cells from patients (22), and the prostate cancer cell line LnCaP (23). Elevated PARP expression has also been shown to be associated with chemoresistance (21). These data further indicate that cancer cells may acquire enhanced PARP activity and pharmacologic inhibition of PARP has been shown to sensitize cancer cells to cancer therapeutics both *in vitro* and in animal models (24-32).

Temozolomide forms methyl adducts in DNA at N^7 guanine, O^6 guanine, and N^3 adenine. Because the methylpurines (N^7-MeG and N^3-MeA) are promptly repaired by the BER system facilitated by PARP-1 and PARP-2, the cytotoxicity is predominantly due to the methylation at the O^6 position of guanine, which is not efficiently repaired. O^6-methylguanine results in a G-T mismatch and activates MMR mechanism, which cleaves off the thymine. The repair system reinserts thymine due to the presence of O^6-methylguanine, resulting in a futile cycle that leads to a persistent strand breakage and ultimately apoptosis (33, 34). PARP inhibition blocks the efficient BER pathway and the high levels of SSB eventually lead to enhanced cell death.

Received 5/23/08; revised 7/10/08; accepted 7/14/08.
The costs of publication of this article were defrayed in part by the payment of page charges. This article must therefore be hereby marked *advertisement* in accordance with 18 U.S.C. Section 1734 solely to indicate this fact.
Requests for reprints: Yan Luo, Cancer Research, GPRD, Abbott Laboratories, 100 Abbott Park Road, Abbott Park, IL 60064. Phone: 847-935-6811; Fax: 847-938-2365. E-mail: yan.luo@abbott.com or Xuesong Liu, Abbott Laboratories, 100 Abbott Park Road, Abbott Park, IL 60064. Phone: 847-938-4409; Fax: 847-938-2365. E-mail: Xuesong.liu@abbott.com

doi:10.1158/1541-7786.MCR-08-0240

We hypothesized that the SSB needs to be converted into a DSB to achieve the maximal cytotoxicity from temozolomide treatment. It was well recognized that the levels of the phosphorylated H2AX (γH2AX) provide a good measurement for DSB (35, 36). γH2AX is an early response to DSB. Upon DSB, the Mre11/Rad50/NBS1 complex is recruited to the DNA damage site, which triggers the activation of ATM (37). The activated ATM phosphorylates Ser^{139} of the carboxyl tail of H2AX, and γH2AX plays an important role in the recruitment of DNA repair proteins such as BRCA1, MDC1, and 53BP1 (38-42). In addition to ATM, ATR and DNA-PKcs are also able to phosphorylate H2AX (41, 43).

ABT-888 potently inhibits the activities of both PARP-1 (K_i = 3.6 nmol/L) and PARP-2 (K_i = 2.9 nmol/L; ref. 44). We studied the effect of ABT-888 on DNA repair and the potentiation of cytotoxicity induced by temozolomide. Our results suggest that the cytotoxicity induced by temozolomide is enhanced preferentially when the repair is delayed by ABT-888 long enough so that the SSBs are converted into DSBs (as measured by γH2AX levels) through DNA replication. Enhancement of antitumor activity of temozolomide by ABT-888 was also shown in melanoma and glioma animal models, representing the two most important clinical indications for temozolomide.

Results

ABT-888 Potentiates the Cytotoxicity of Temozolomide in Human Tumor Cell Lines

We have developed a series of benzimidazole compounds that are potent inhibitors of PARP. ABT-888 is an orally active compound with good pharmacokinetic properties (44). ABT-888 inhibits PAR formation in cells with an EC_{50} of 4.5 nmol/L (data not shown). We studied the combination of temozolomide with ABT-888 in detail. Two-way titration of both temozolomide and ABT-888 showed that 50 nmol/L of ABT-888 started to potentiate temozolomide significantly and the maximal potentiation was achieved at 5 μmol/L of ABT-888 before significant cytotoxicity was induced by ABT-888 alone. Cell growth inhibition by temozolomide was potentiated with a maximal potentiation factor (PF_{50}) of 14.6-fold by ABT-888 (Fig. 1A).

Because the levels of γH2AX reflect the levels of double-stranded DNA breaks, we also examined the levels of γH2AX in the temozolomide-treated cells. Cells are treated with temozolomide first for 30 minutes and the extent of DNA repair 1 hour after the temozolomide treatment is monitored by γH2AX signal. The γH2AX signal was low in cells treated with ABT-888 or temozolomide alone as single agents. The addition of ABT-888 increased dramatically the γH2AX levels in temozolomide-treated cells, indicating the effect of ABT-888 to delay DNA repair. Titration of ABT-888 in the γH2AX assay also showed that the effective dose concentration of ABT-888 in delaying DNA repair is the same as that for the potentiation of the cytotoxicity of temozolomide (Fig. 1B and C).

Potentiation of Temozolomide Cytotoxicity by PARP Inhibitor ABT-888 Requires a Conversion of ssDNA Damages to DSBs

We examined the effect of drug exposure on the extent of cytotoxicity. HCT116 cells were treated with temozolomide plus ABT-888 for different lengths of time and then cells were further incubated in medium without any drugs for the rest of the remaining 5-day incubation time. As shown in Fig. 2A, a 17-hour drug exposure is sufficient to achieve the maximal potentiation effect (data not shown for 48 and 120 hours). In a similar experiment where the γH2AX signals were measured, γH2AX signals reached the maximal level after a 17-hour incubation, correlating with the Alamar blue assay results (Fig. 2B). To rule out the possibility that the increase of the γH2AX signal is due to apoptosis, Z-VAD was included in the incubation in this experiment. We also investigated whether apoptosis was induced in HCT116 cells treated with temozolomide/ABT-888 by caspase activity assay. As shown in Fig. 2C, low caspase activities were observed in cells treated with DMSO, 0.1 mmol/L, or 0.3 mmol/L temozolomide. However, significant caspase activities were observed in cells treated with 1 mmol/L temozolomide or all three doses of temozolomide in the presence of ABT-888 (Fig. 2C). Inclusion of Z-VAD completely inhibited caspase activity (data not shown).

Our data indicated that ABT-888 facilitates the conversion of temozolomide-induced SSB to DSB in HCT116 cells. We further tested this hypothesis in the following experiment. Synchronized HCT116 spend ~12 hours in G_1 and ~8 to 10 hours in the S phase (Supplementary Data 1). HCT116 cells were synchronized in G_0 by serum starvation and released in the medium with serum. In treatment I, the cells were released in the medium with serum for 11 hours to allow cells to progress through most of the G_1 phase. The cells were then treated with temozolomide and ABT-888 for 7 hours, and, thus, the drug exposure occurs during the S phase to allow any SSB to be converted into DSB. In treatment II, the cells were treated with temozolomide and ABT-888 for 7 hours immediately after being released from serum starvation, and, thus, the whole drug exposure occurred during the early G_1 phase. The cells were then incubated in the medium without drugs to allow DNA repair for several hours before they progress into S phase. γH2AX measurements indicated that treatment I produced a much higher level of DSB in temozolomide-ABT-888 combination than treatment II (Fig. 3A). Consistent with this result, 5 μmol/L of ABT-888 potentiates temozolomide by 10.3-fold in treatment I compared with 2.8-fold in treatment II (Fig. 3B). A similar effect was observed in HeLa cells released from either double thymidine block or nocodazole block (Fig. 3C and D). To confirm that ABT-888 potentiates the effect of temozolomide through its ability to convert SSBs to DSBs during S-phase DNA replication, we conducted neutral comet assay on synchronized HeLa cells treated with temozolomide or temozolomide/ABT-888. The neutral comet assay mainly detects DSBs. As shown in Fig. 3E, only the combination treatment induced significant comet tail. These results suggest that a conversion of SSB into DSB through DNA replication probably enhances the temozolomide-induced cytotoxicity. These results also suggest that we should select those PARP inhibitors that have long drug exposure *in vivo* to achieve optimal antitumor activity.

ABT-888 Potentiates the Antitumor Activity by Temozolomide in Animal Models

The two most important clinical indications of temozolomide are melanoma and glioblastoma. Therefore, we measured

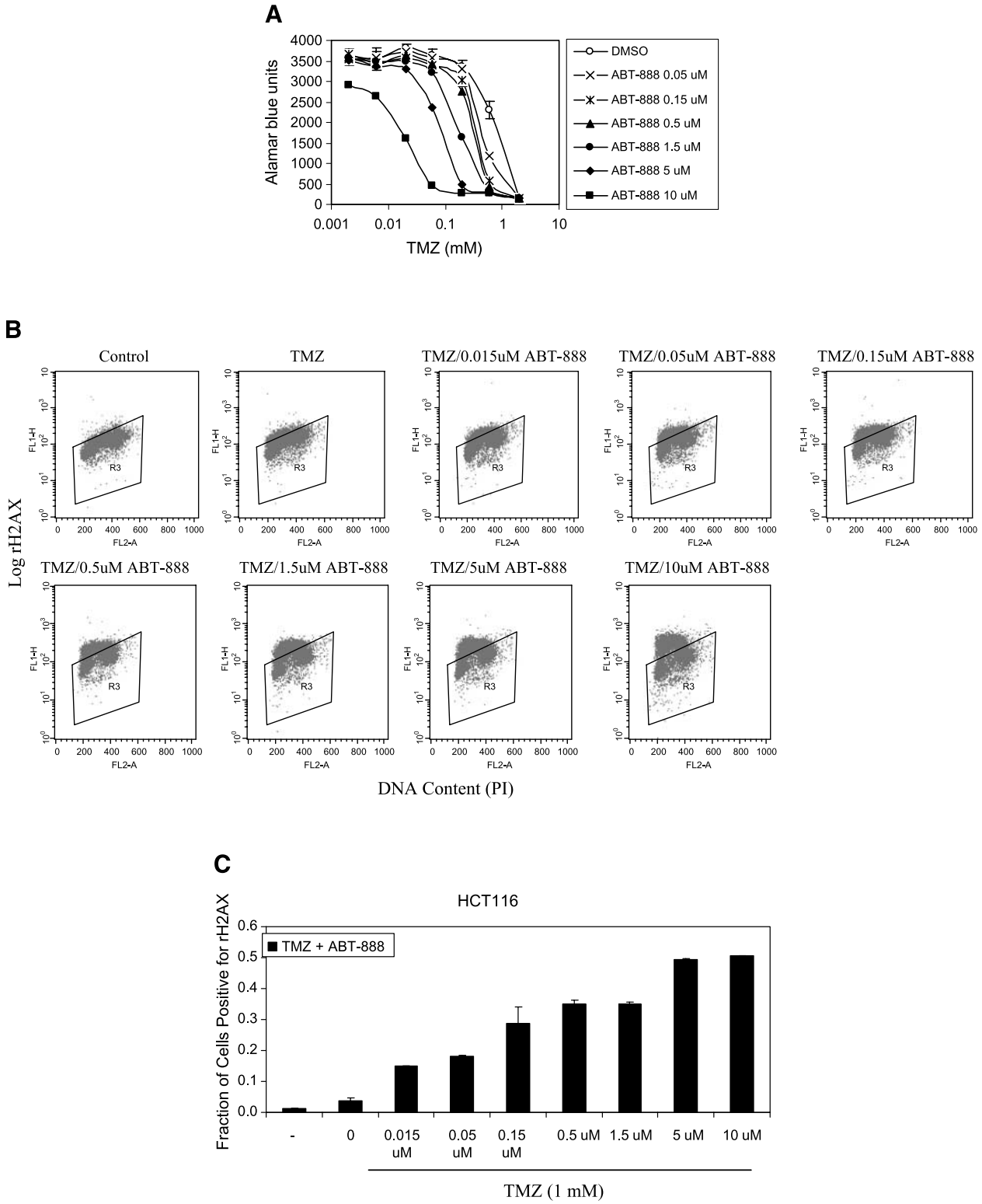

FIGURE 1. ABT-888 potentiates temozolomide activity in HCT116 cells. **A.** Potentiation assay was carried out as described in Materials and Methods. The concentration of ABT-888 in each temozolomide (*TMZ*) titration curve is indicated at the right of the graph. **B.** γH2AX assay was carried out as described in Materials and Methods. The gate setting was based on the control sample where all the cells were included in the gated area. The same gate setting was then applied to the treated samples. The γH2AX-positive cells were scored as those that fall outside the gated area, the portion of which is indicated above the histogram within each graph. The concentration of ABT-888 (μmol/L) in each treatment is indicated above each graph. PI, propidium iodide. **C.** γH2AX levels in combinations with different concentrations of ABT-888 and temozolomide. The concentration of ABT-888 (μmol/L) in each treatment is indicated below each bar graph.

the efficacy of ABT-888 to potentiate temozolomide in a B16F10 melanoma syngeneic model and an orthotopic rat 9L glioma model.

B16F10 murine melanoma was chosen because it represents a clinically relevant cancer that is relatively insensitive to most chemotherapeutics. Furthermore, the B16F10 model has modest sensitivity to temozolomide therapy that recapitulates the human clinical situation. ABT-888 inhibits PARP in B16F10 cells with an EC_{50} of 0.6 nmol/L. It potentiates temozolomide in delaying DNA repair and reducing cell survival in a similar fashion as in HCT116 cells (Fig. 4A and B). ABT-888, administered orally, significantly potentiates the temozolomide efficacy in a dose-dependent manner. The combinations of ABT-888 at 25 and 5 mg/kg/d with temozolomide were significantly more efficacious than temozolomide monotherapy ($P < 0.05$; Fig. 5A). No increased toxicity was observed at these doses of ABT-888 + temozolomide (data not shown). We have developed an ELISA that can detect the formation of PAR in cells and tumors and the PAR ELISA assay was used to monitor the PARP inhibition in tumors. Tumors from different treatment groups were harvested 24 hours after the last dosing and PAR levels were measured. ABT-888 exhibited dose-dependent reduction in PAR levels even at 24 hours post dosing, indicating the PARP inhibition in tumors at the efficacious dose (Fig. 5B). Consistent with this result, we also observed significant levels of ABT-888 accumulated in B16F10 tumors 24 hours post dosing (data not shown), providing long enough exposure of ABT-888 to achieve maximal potentiation of temozolomide.

ABT-888 readily crosses the blood-brain barrier (44). Therefore, we tested its efficacy in potentiating temozolomide in an orthotopic glioma model, another important temozolomide indication in clinic. To mimic the clinical setting, the efficacy was tested in rat 9L orthotopic glioma model and the tumor growth was monitored with magnetic resonance imaging. In this model, ABT-888 enhances the antitumor activity of temozolomide. As single-agent treatment, neither temozolomide (17.5 mg/kg, qd) nor ABT-888 (25 mg/kg, bd) has significant efficacy. However, the combination treatment of the two agents together reduced tumor growth by 60%, 67%, and 52% more when compared with that of temozolomide treated group on days 8, 11, and 14, respectively (Fig. 6).

Discussion

PARP is involved predominantly in single-strand DNA repair, especially through the BER pathway. In this process, the DNA lesion is recognized by DNA glycosylase, which hydrolyzes the modified base to yield an apurinic-apyrimidinic

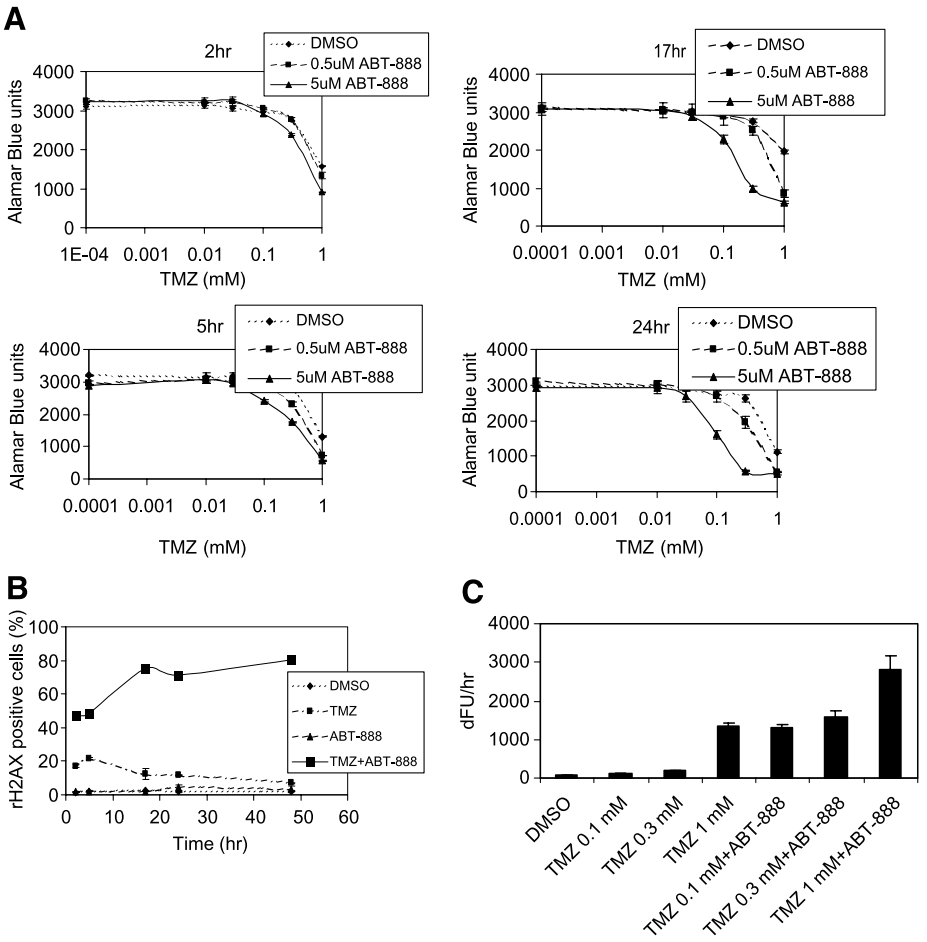

FIGURE 2. DSB converted from the SSB is more effective in inducing cytotoxicity. **A.** HCT116 cells were treated with temozolomide and/or ABT-888 at the indicated concentrations for the indicated time period, followed by incubation with complete medium without drugs for a total time of 5 d. **B.** HCT116 cells were treated with 1 mmol/L temozolomide, 5 μmol/L ABT-888, or the combination of temozolomide and ABT-888 in the presence of Z-VAD for the indicated time period. Cells were harvested and analyzed for γH2AX assay. **C.** HCT116 cells were treated with the indicated concentration of temozolomide in the absence or presence of 5 μmol/L ABT-888 for 3 d. Caspase activity assay was carried out as described in Materials and Methods.

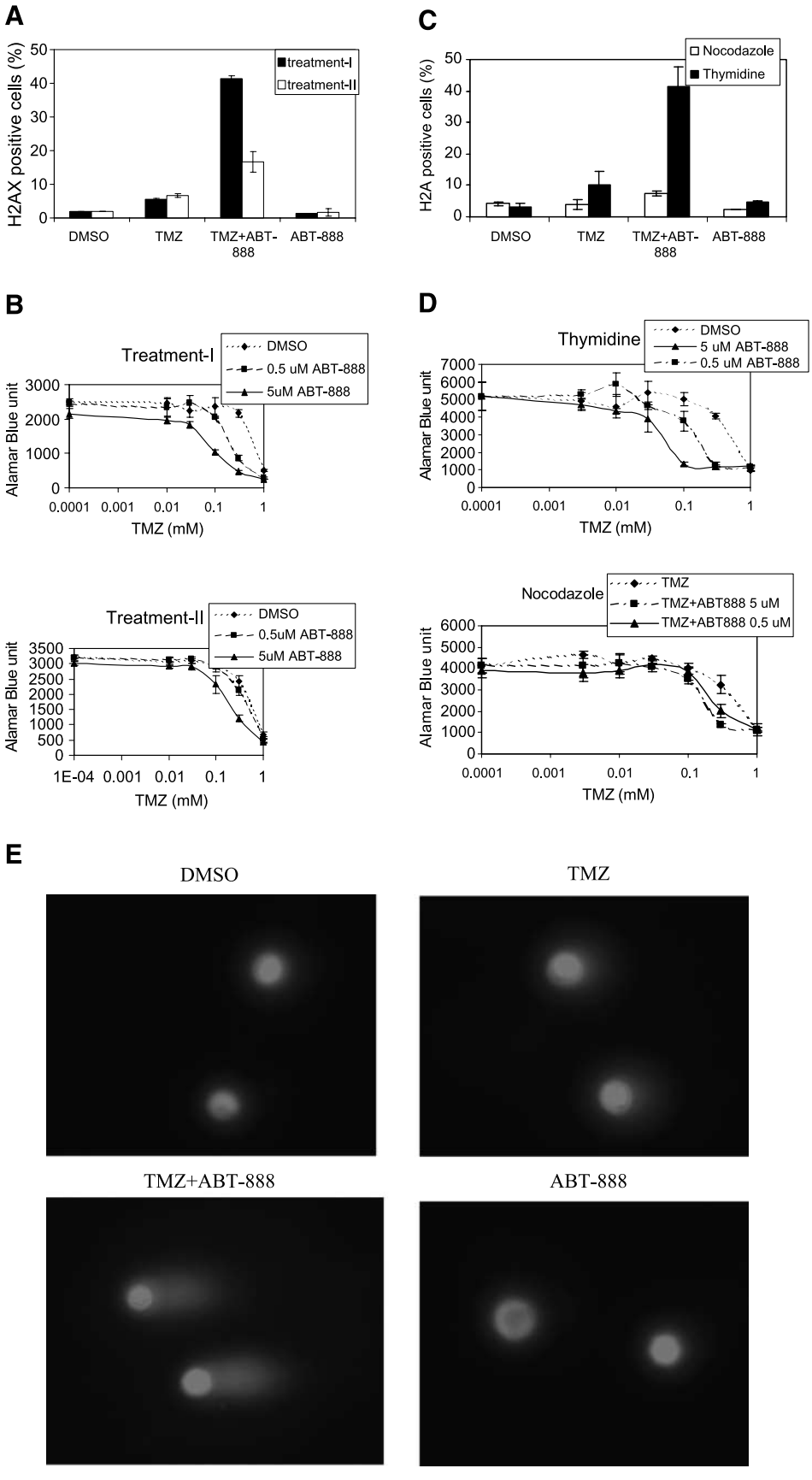

FIGURE 3. ABT-888 facilitates the conversion of temozolomide-induced ssDNA damages to DSBs. **A** and **B.** HCT116 cells were serum starved for 48 h, then the cells were either cultured in complete medium for 11 h (treatment I) or directly (treatment II) treated with 1 mmol/L temozolomide alone, 5 μmol/L ABT-888 alone, or temozolomide+ABT-888 for 7 h. The cells were harvested immediately for the γH2AX assay (**A**) or cultured in medium without drugs for a total incubation time of 5 d for the Alamar blue assay (**B**). **C** and **D.** HeLa cells were arrested with either double thymidine block or nocodazole as described in Materials and Methods. Then, the cells were released in complete medium for 3.5 h (nocodazole) or 2 h (thymidine) followed by the treatment with 1 mmol/L temozolomide or temozolomide in combination with ABT-888 for 6 h. Cells were either harvested immediately for γH2AX assay (**C**) or cultured in medium without drugs for a total incubation time of 5 d for Alamar blue assay (**D**). **E.** HeLa cells were synchronized at the S phase with 2.5 mmol/L thymidine for 16 h. The cells were washed with PBS and released in complete medium for 2 h. Then, the cells were treated with DMSO, 1 mmol/L temozolomide, 5 μmol/L ABT-888, or 1 mmol/L temozolomide/5 μmol/L ABT-888 for 30 min. The cells were further incubated with either DMSO or 5 μmol/L ABT-888 for another 1 h. Comet assay was carried out as described in Materials and Methods. Representative images were shown.

(AP) base. The AP base is then removed by AP endonuclease to generate a nick in the DNA. PARP-1 binds to the nick and recruits DNA polymerase β (Pol β) and the DNA ligase III-XRCC1 complex (7, 45, 46) for the repair. Normally, temozolomide forms methyl adducts in DNA at N^7 guanine, O^6 guanine, and N^3 adenine. Because the methylpurines (N^7-MeG and N^3-MeA) are promptly repaired by the BER system, the cytotoxicity is predominantly due to the methylation at the O^6 position of guanine, which is not efficiently repaired through MMR system. However, cells defective in the MMR system are unable to generate the persistent strand breaks and are thus resistant to temozolomide. PARP inhibitors inhibit PARP1 and PARP2, block the BER pathway, and sensitize the MMR-deficient cells to temozolomide (11-13), providing a potentially very effective combination therapy with temozolomide for cancer patients with MMR defects.

We have explored the mechanism of potentiation of temozolomide cytotoxicity by the PARP inhibitor ABT-888. Temozolomide activity is potentiated very well by ABT-888. We showed that in unsynchronized cells, a minimum of 17 to 24 hours of exposure of ABT-888 is required to achieve the maximal potentiation (Fig. 2A). By contrast, in synchronized cells, only 7 hours of ABT-888 exposure is sufficient to efficiently potentiate temozolomide cytotoxicity when the treatment times overlap during the S phase of the cell cycle. However, the temozolomide/ABT-888 treatment during the G_1 phase generates much less cytotoxicity (Fig. 3). We hypothesized that the temozolomide-induced methylated nucleotides were not efficiently repaired because the BER system was blocked by ABT-888. The accumulated SSBs were then further converted into DSBs during the S phase. Indeed, the DNA DSB levels, as measured by γH2AX levels, were much higher when the temozolomide/ABT-888 treatment occurs during the S phase (Fig. 3). The increased level of DSB correlated with the higher level of cytotoxicity under this condition (Fig. 3). Therefore, in an unsynchronized cell population, similar to the *in vivo* situation, the requirement for a long incubation of ABT-888 may reflect the requirement to maintain the high levels of SSB long enough to be converted into DSB via DNA replication.

A similar concept was introduced by Bryant and Helleday where they proposed that PARP inhibition leads to defect in repair of endogenous SSBs, which, in turn, cause collapses in DNA replication forks (14). The increase of γH2AX levels upon PARP inhibition was also shown in combination studies with irradiation, used in this case as a general indicator of DNA damage (47). However, the current report provides the first mechanistic study regarding the importance of DSB for temozolomide-induced cytotoxicity. At the same time, our studies showed the utility of γH2AX levels as a valid measurement for the effect of PARP inhibition on DNA repair.

Two main indications of temozolomide in the clinic are the treatments for melanoma and glioblastoma. We have tested the potentiation of temozolomide by ABT-888 in these tumor types *in vivo*. ABT-888 significantly enhanced the antitumor activity of temozolomide in both the syngeneic melanoma model in mice and the orthotopic glioma model in rat. Based on our study, a PARP inhibitor that has a long half-life or can accumulate for a long period of time in tumors is preferred for optimal potentiation of temozolomide. Indeed, that is what we observed with ABT-888 *in vivo* (Fig. 5B). In the B16F10 melanoma model, we have also shown that ABT-888 inhibits PAR formation in tumors at the efficacious dose even at 24 hours post dosing, indicating the mechanism-based efficacy. These preclinical results provide a scientific rationale for developing ABT-888 as a chemosensitizer of temozolomide for melanoma and glioma patients in the clinical setting. ABT-888 has good pharmacokinetic profile across species, especially that it can cross the blood-brain barrier (44). The favorable pharmacokinetic profile makes ABT-888 particularly suitable for combination therapy with temozolomide to treat patients with intracranial tumors in clinic. ABT-888 is currently in phase 1 trials in patients with melanoma and glioblastoma.

Materials and Methods

Cell Lines

HCT116 colon carcinoma, HeLa cervical carcinoma, and B16F10 melanoma lines were purchased from the American Type Cell Collection. All chemicals and Z-VAD were obtained from Sigma. The caspase-3 substrate Ac-DEVD-FMK was purchased from Bachem. Temozolomide was obtained from Dik Drug Co.

Caspase-3 Activity Assay

Two million HCT116 cells were plated in a 10-cm culture dish. The cells were treated with the indicated concentrations of

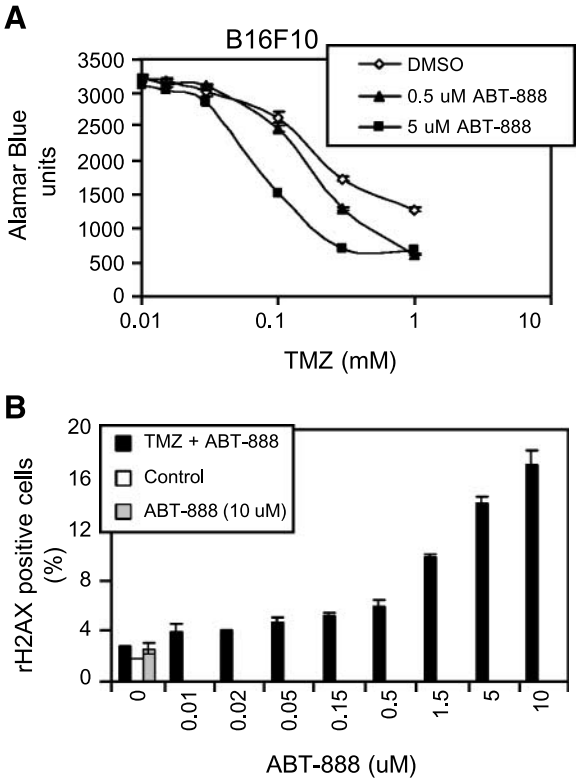

FIGURE 4. ABT-888 potentiates the activity of temozolomide in murine B16F10 melanoma cells. **A.** Potentiation assay was carried out in B16F10 cells in a 96-well plate with 500 cells per well for 5 d. **B.** B16F10 cells were treated with the indicated concentrations of temozolomide and ABT-888. γH2AX assay was carried out as described in Materials and Methods.

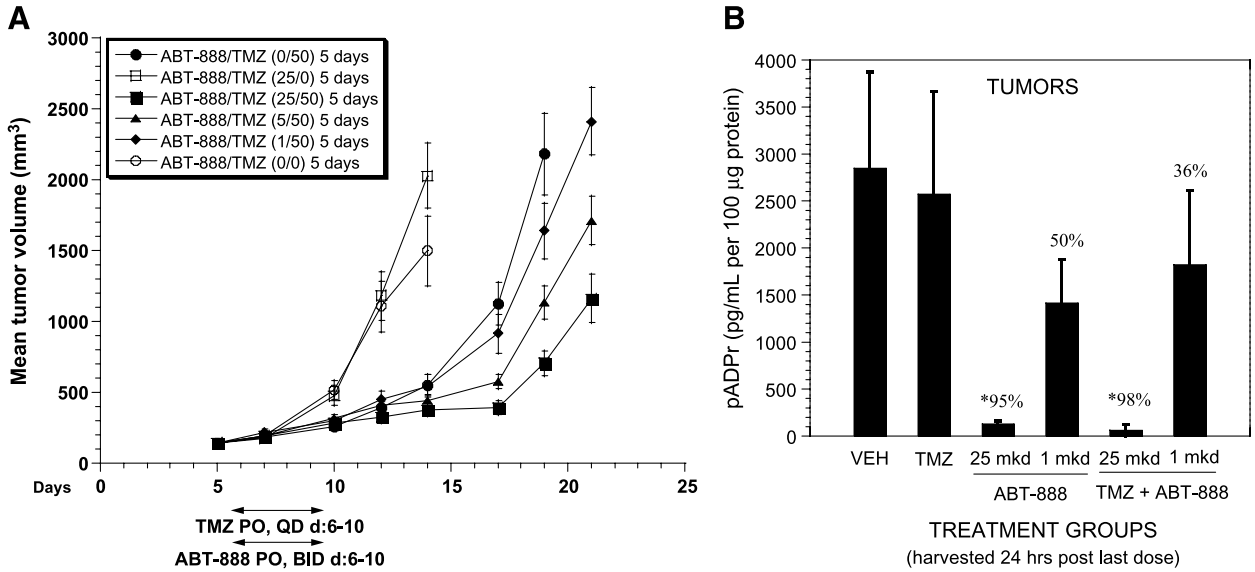

FIGURE 5. ABT-888 enhances the antitumor activity of temozolomide in murine B16F10 melanoma. **A.** ABT-888 enhances the antitumor activity of temozolomide in the B16F10 *in vivo* model. Temozolomide was administered on an oral, qd × 5 schedule on days 6 to 10 at 50 mg/kg/d concurrently with ABT-888 on an oral, bd × 5 schedule at 25, 5, and 1 mg/kg/d. The experiment consists of 10 mice per treatment group; bars, SE. **B.** ABT-888 inhibits PARP activity at the efficacious dose measured by PAR ELISA assay. Mice were treated as summarized in **A**. Tumor samples were harvested 24 h post last dosing and processed for PAR assay as described in Materials and Methods. Columns, mean pADPr (n = 4 or 5 mice per treatment group); bars, SE. The percentages of inhibition versus vehicle control are indicated above each bar. *, $P < 0.05$.

temozolomide or the combination of temozolomide and ABT-888. After 3 d, cells were harvested. Six thousand cells from each treatment condition were diluted in 100 µL culture medium and placed into 96-well plate in triplicates. Caspase-3 activity assay was carried out as described using the substrate Ac-DEVD-FMK (48).

Cell Cycle Synchronization

HCT116 cells were serum starved for 48 h (G_0). HeLa cells were treated with nocodazole (100 ng/mL) for 12 h (G_2). A double thymidine block was used to synchronize cells in the S phase. Cells were treated with 2 mmol/L thymidine for 16 h and released for 8 h, followed by an additional 16-h thymidine block. The cells were then washed thrice with PBS and released into complete medium. Cell cycle arrest was confirmed by flow cytometry analysis (BD Biosciences).

γH2AX Assay

Human cancer cells were pretreated with ABT-888 for 30 min, then with DNA-damaging agents for 30 min, followed by incubation with ABT-888 for an additional 1 hour to allow DNA repair. After the treatment, the cells were fixed with 250 µL of BD Cytofix/Cytoperm solution (BD Biosciences) at room temperature for 20 min followed by three times washing with 1× BD Perm/Wash Solution (BD Biosciences). After blocking with 3% bovine serum albumin for 30 min, the cells were incubated with the following antibodies in Perm/Wash solution with washes in between: mouse anti–phospho-histone γH2AX antibody (1:250; Upstate Biotechnologies) and Alexa 488 goat anti-mouse IgG(H+L)F(ab′)2 fragment conjugate (1:200; Invitrogen). The DNA was immunostained with 50 µg/mL propidium iodide in staining buffer [PBS without Mg^{2+} or Ca^{2+}, 1% heat-inactivated FCS, 0.09% (w/v) sodium azide (pH 7.4-7.6)] for 10 min in the dark. Immunologic flow cytometry was done to quantify the γH2AX signal. Each data point is the average of two values. Error bars represent the SD.

Potentiation Assay

Cells were plated at 750 per well in a 96-well plate. Cells were then cotreated with cytotoxic agents and PARP inhibitors for 5 d. Alamar blue assay was carried out as per the manufacturer's instructions (Biosource, Intl., Inc.). Briefly, the medium was removed from the plate, and 100 µL of Alamar blue solution (10% Alamar blue in complete culture medium)

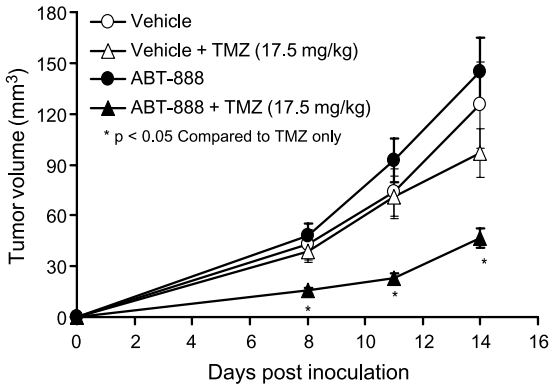

FIGURE 6. ABT-888 enhances the antitumor activity of temozolomide in the rat 9L glioma orthotopic model. Tumor cells were inoculated into rat brain as described in Materials and Methods. The vehicle for the temozolomide and ABT-888 was saline. ABT-888 was administered at 25 mg/kg/dose, bd, orally, on days 2 to 17. Starting on day 4, temozolomide was administered at 17.5 mg/kg, qd, orally, on day 4 to 8 at 2 h post the morning dose of ABT-888.

were added to each well. After 3 h, the plate was read on an *fmax* Fluorescence Microplate Reader (Molecular Devices), set at the excitation wavelength of 544 nm and emission wavelength of 595 nm. Data were analyzed using SOFTmax PRO software. Each data point is the average of three values. Error bars represent the SD.

PAR ELISA

pADPr levels in tumors were analyzed by sandwich ELISA. Tumors were excised from euthanized mice treated *in vivo* and protein lysates were prepared as described (44). Immunoplates (Pierce Endogen) were coated with anti-PAR monoclonal antibody (Trevigen) in 0.1 mol/L carbonate buffer (pH 9.5) for 2 h at 37°C. Plates were washed five times in TBS-0.05% Tween 20/TBST and blocked for 1 h at room temperature with Superblock (Pierce Endogen). Samples and standards (purified PAR polymers; BioMol) were incubated overnight at 37°C, followed by incubation with a rabbit polyclonal anti-PAR antibody (Trevigen) and subsequently a horseradish peroxidase–conjugated secondary antibody (KPL). The signal was developed using a SuperSignal Femto for ELISA (Pierce Endogen). Plates were read using a Spectramax EM plate reader (Molecular Devices). Each data point is the average of three values. Error bars represent the SD.

B16F10 Syngeneic Melanoma In vivo *Model*

All animal studies were conducted in accordance with the guidelines established by the internal Institutional Animal Care and Use Committee. ABT-888 was delivered in a vehicle containing 0.9% NaCl adjusted to pH 4.0. Temozolomide (Schering-Plough) was formulated using 0.2% hydroxypropyl methylcellulose. B16F10 cells (6×10^4) were injected s.c. into the flank of female C57BL/6 mice (Charles River Laboratories) as previously described (44). Tumors were measured using two bisecting diameters and tumor volumes were calculated by $(L \times W^2)/2$. Mean percentage treated versus control was plotted and groups were compared by the Student's *t* test (two-tailed) to determine statistical significance ($P < 0.05$; StatView software, SAS Institute).

9L Orthotopic Glioma Model

Female Fischer 344 rats (Charles River Laboratories) were anesthetized with ketamine (80-100 mg/kg, i.p.) and xylazine (8-10 mg/kg, i.p.). Ten microliters of cell suspension containing 5×10^5 tumor cells were injected at 2 mm anterior and 2 mm lateral to bregma and 3 mm deep into right hemisphere of each rat brain. The burr hole was bone wax-sealed to reduce extracerebral leakage. The incision was closed with veterinary adhesive and rats were allowed to recover. Tumor growth was evaluated using multislice contrast enhanced magnetic resonance imaging with a contrast agent, Magnevist (Bayer HealthCare Pharmaceuticals) on 8, 11, and 14 d post tumor inoculation. One-way ANOVA followed by a Dunnett's test was done to compare the tumor volumes between each treatment group and the vehicle group.

Comet Assay

Neutral comet assay kit was purchased from Trevigen and the assay was carried out according to the manufacturer's instruction. Briefly, the cells were harvested and combined with LMAgarose. Seventy-five microliters of the mixture were applied to a Comet slide and kept at 4°C in the dark for 10 min. The slides were immersed in prechilled lysis buffer and left on ice for 30 min. The slides were washed with Tris-borate EDTA and placed flat onto a gel tray in a horizontal electrophoresis apparatus. Electrophoresis was carried out by applying 16 V for 25 min. The slides were washed with water and immersed in 70% ethanol for 5 min. The samples were left in air overnight. Fifty microliters of SYBR green were placed onto each sample. Images of the comet assay were photographed with an Axiovert 200M microscope (Carl Zeiss, Inc.).

Disclosure of Potential Conflicts of Interest

The authors disclosed no conflict of interest.

References

1. Chambon P, Weill JD, Mandel JL. Nicotinamede mononucleotide activation of a new DNA-dependent poly-adenylic acid synthesizing enzyme. Biochem Biophys Res Commun 1963;11:39–43.

2. Amé Jean C, Spenlehauer C, de Murcia G. The PARP superfamily. Bioessays 2004;26:882–93.

3. Tulin A, Spradling A. Chromatin loosening by poly(ADP)-ribose polymerase (PARP) at *Drosophila* puff loci. Science 2003;299:560–2.

4. Kraus WL, Lis John T. PARP goes transcription. Cell 2003;113:677–83.

5. Tentori L, Portarena I, Graziani G. Potential clinical applications of poly(ADP-ribose)polymerase (PARP) inhibitors. Pharmacol Res 2002;45:73–85.

6. Ménissier de Murcia J, Niedergang C, Trucco C, et al. Requirement of poly(ADP-ribose) polymerase in recovery from DNA damage in mice and in cells. Proc Natl Acad Sci U S A 1997;94:7303–7.

7. Schreiber V, Amé Jean C, Dollé P, et al. Poly(ADP-ribose) polymerase-2 (PARP-2) is required for efficient base excision DNA repair in association with PARP-1 and XRCC1. J Biol Chem 2002;277:23028–36.

8. Ménissier de Murcia J, Ricoul M, Tartier L, et al. Functional interaction between PARP-1 and PARP-2 in chromosome stability and embryonic development in mouse. EMBO J 2003;22:2255–63.

9. Virág L, Szabó C. The therapeutic potential of poly(ADP-ribose) polymerase inhibitors. Pharmacol Rev 2002;54:375–429.

10. Pleschke JM, Kleczkowska HE, Strohm M, Althaus FR. Poly(ADP-ribose) binds to specific domains in DNA damage checkpoint proteins. J Biol Chem 2000;275:40974–80.

11. Curtin NJ, Wang L-Z, Yiakouvaki A, et al. Novel poly(ADP-ribose)polymerase-1 inhibitor, AG-14361, restores sensitivity to temozolomide in mismatch repair-deficient cells. Clin Cancer Res 2004;10:881–9.

12. Liu L, Taverna P, Whiteacre CM, Chatterjee S, Gerson SL. Pharmacologic disruption of base excision repair sensitizes mismatch repair-deficient and proficient colon cancer cells to methylating agents. Clin Cancer Res 1999;5:2908–17.

13. Cheng CL, Johnson Stewart P, Keir Stephen T, et al. Poly(ADP-ribose) polymerase-1 inhibition reverses temozolomide resistance in a DNA mismatch repair-deficient malignant glioma xenograft. Molecular cancer therapeutics. Mol Cancer Ther 2005;4:1364–8.

14. Bryant HE, Helleday T. Inhibition of poly (ADP-ribose) polymerase activates ATM which is required for subsequent homologous recombination repair. Nucleic Acids Res 2006;34:1685–91.

15. Hochegger H, Dejsuphong D, Fukushima T, et al. Parp-1 protects homologous recombination from interference by Ku and Ligase IV in vertebrate cells. EMBO J 2006;25:1305–14.

16. Wang M, Wu W, Wu W, et al. PARP-1 and Ku compete for repair of DNA double strand breaks by distinct NHEJ pathways. Nucleic Acids Res 2006;34:6170–82.

17. Tomoda T, Kurashige T, Moriki T, Yamamoto H, Fujimoto S, Taniguchi T. Enhanced expression of poly(ADP-ribose) synthetase gene in malignant lymphoma. Am J Hematol 1991;37:223–7.

18. Wielckens K, Garbrecht M, Kittler M, Hilz H. ADP-ribosylation of nuclear proteins in normal lymphocytes and in low- grade malignant non-Hodgkin lymphoma cells. Eur J Biochem 1980;104:279–87.

19. Nomura F, Yaguchi M, Togawa A, et al. Enhancement of poly-adenosine diphosphate-ribosylation in human hepatocellular carcinoma. J Gastroenterol Hepatol 2000;15:529–35.

20. Shiobara M, Miyazaki M, Ito H, et al. Enhanced polyadenosine diphosphate-ribosylation in cirrhotic liver and carcinoma tissues in patients with hepatocellular carcinoma. J Gastroenterol Hepatol 2001;16:338–44.

21. Kubo S, Matsutani M, Nakagawa K, Ogura T, Esumi H, Saijo N. Participation of poly(ADP-ribose) polymerase in the drug sensitivity in human lung cancer cell lines. J Cancer Res Clin Oncol 1992;118:244–8.

22. Fukushima M, Kuzuya K, Ota K, Ikai K. Poly(ADP-ribose) synthesis in human cervical cancer cell-diagnostic cytological usefulness. Cancer Lett 1981; 14:227–36.

23. McNealy T, Frey M, Trojon L, Knoll T, Alken P, Michel Maurice S. Intrinsic presence of poly (ADP-ribose) is significantly increased in malignant prostate compared to benign prostate cell lines. Anticancer Res 2003;23:1473–8.

24. Curtin NJ, Wang LZ, Yiakouvaki A, et al. Novel poly(ADP-ribose) polymerase-1 inhibitor, AG14361, restores sensitivity to temozolomide in mismatch repair-deficient cells. Clin Cancer Res 2004;10:881–9.

25. Delaney CA, Wang LZ, Kyle S, et al. Potentiation of temozolomide and topotecan growth inhibition and cytotoxicity by novel poly(adenosine diphosphoribose) polymerase inhibitors in a panel of human tumor cell lines. Clin Cancer Res 2000;6:2860–7.

26. Miknyoczki SJ, Jones Bolin S, Pritchard S, et al. Chemopotentiation of temozolomide, irinotecan, and cisplatin activity by CEP-6800, a poly(ADP-ribose) polymerase inhibitor. Mol Cancer Ther 2003;2:371–82.

27. Tentori L, Leonetti C, Scarsella M, et al. Systemic administration of the PARP inhibitor GPI 15427 increases the anti-tumor activity of temozolomide in melanoma, glioma and lymphoma preclinical models in vivo. Proc Am Assoc Cancer Res Annu Meet 2003;44:1088–9.

28. Tentori L, Leonetti C, Scarsella M, et al. Combined treatment with temozolomide and poly(ADP-ribose) polymerase inhibitor enhances survival of mice bearing hematologic malignancy at the central nervous system site. Blood 2002;99:2241–4.

29. Tentori L, Leonetti C, Scarsella M, et al. Systemic administration of GPI 15427, a novel poly(ADP-ribose) polymerase-1 inhibitor, increases the antitumor activity of temozolomide against intracranial melanoma, glioma, lymphoma. Clin Cancer Res 2003;9:5370–9.

30. Calabrese CR, Almassy R, Barton S, et al. Anticancer chemosensitization and radiosensitization by the novel poly (ADP-ribose) polymerase-1 inhibitor AG14361. J Natl Cancer Inst 2004;96:56–67.

31. Calabrese CR, Batey MA, Thomas HD, et al. Identification of potent nontoxic poly(ADP-ribose) polymerase-1 inhibitors: chemopotentiation and pharmacological studies. Clin Cancer Res 2003;9:2711–8.

32. Veuger SJ, Curtin NJ, Richardson CJ, Smith GCM, Durkacz BW. Radiosensitization and DNA repair inhibition by the combined use of novel inhibitors of DNA-dependent protein kinase and poly(ADP-ribose) polymerase-1. Cancer Res 2003;63:6008–15.

33. D'Atri S, Tentori L, Lacal PM, et al. Involvement of the mismatch repair system in temozolomide-induced apoptosis. Mol Pharmacol 1998;54:334–41.

34. Plummer ER, Middleton MR, Jones C, et al. Temozolomide pharmacodynamics in patients with metastatic melanoma: DNA damage and activity of repair enzymes O^6-alkylguanine alkyltransferase and poly(ADP-ribose) polymerase-1. Clin Cancer Res 2005;11:3402–9.

35. Taneja N, Davis M, Choy JS, et al. Histone H2AX phosphorylation as a predictor of radiosensitivity and target for radiotherapy. J Biol Chem 2004;279: 2273–80.

36. Olive PL, Banáth JP, Sinnott LT. Phosphorylated histone H2AX in spheroids, tumors, and tissues of mice exposed to etoposide and 3-amino-1,2,4-benzotriazine-1,3-dioxide. Cancer Res 2004;64:5363–9.

37. Bakkenist CJ, Kastan MB. DNA damage activates ATM through intermolecular autophosphorylation and dimer dissociation. Nature 2003;421: 499–506.

38. Burma S, Chen BP, Murphy M, Kurimasa A, Chen DJ. ATM phosphorylates histone H2AX in response to DNA double-strand breaks. J Biol Chem 2001;276: 42462–7.

39. Lukas C, Melander F, Stucki M, et al. Mdc1 couples DNA double-strand break recognition by Nbs1 with its H2AX-dependent chromatin retention. EMBO J 2004;23:2674–83.

40. Paull TT, Rogakou EP, Yamazaki V, Kirchgessner CU, Gellert M, Bonner WM. A critical role for histone H2AX in recruitment of repair factors to nuclear foci after DNA damage. Curr Biol 2000;10:886–95.

41. Ward IM, Chen J. Histone H2AX is phosphorylated in an ATR-dependent manner in response to replicational stress. J Biol Chem 2001;276: 47759–62.

42. Rogakou EP, Pilch DR, Orr AH, Ivanova VS, Bonner WM. DNA double-stranded breaks induce histone H2AX phosphorylation on serine 139. J Biol Chem 1998;273:5858–68.

43. Stiff T, Mark OD, Rief N, Iwabuchi K, Löbrich M, Jeggo PA. ATM and DNA-PK function redundantly to phosphorylate H2AX after exposure to ionizing radiation. Cancer Res 2004;64:2390–6.

44. Donawho CK, Luo Y, Luo Y, et al. ABT-888, an orally active poly(ADP-ribose) polymerase inhibitor that potentiates DNA-damaging agents in preclinical tumor models. Clin Cancer Res 2007;13:2728–37.

45. Dianov GL, KM SD II, Allison SL. Repair of abasic sites in DNA. Mutat Res 2003;531:157–63.

46. Masson M, Niedergang C, Schreiber V, Muller S, Menissier de Murcia J, de Murcia G. XRCC1 is specifically associated with poly(ADP-ribose) polymerase and negatively regulates its activity following DNA damage. Mol Cell Biol 1998;18:3563–71.

47. Albert JM, Cao CX, Kim KW, et al. Inhibition of poly(ADP-ribose) polymerase enhances cell death and improves tumor growth delay in irradiated lung cancer models. Clin Cancer Res 2007;13:3033–42.

48. Liu X, Shi Y, Han EK, et al. Downregulation of Akt1 inhibits anchorage-independent cell growth and induces apoptosis in cancer cells. Neoplasia 2001;3: 278–86.

Molecular Cancer Research

Potentiation of Temozolomide Cytotoxicity by Poly(ADP)Ribose Polymerase Inhibitor ABT-888 Requires a Conversion of Single-Stranded DNA Damages to Double-Stranded DNA Breaks

Xuesong Liu, Yan Shi, Ran Guan, et al.

Mol Cancer Res 2008;6:1621-1629.